Co-culture of chondrons and mesenchymal stromal cells reduces the loss of collagen VI and improves extracellular matrix production

Owida HA[1], Ruiz TH[1], Dhillon A[1], Yang Y [1]*, Kuiper NJ [1,2]

[1]Institute of Science & Technology in Medicine, University of Keele, Stoke-on-Trent, ST4 7QB, UK

[2]Arthritis Research Centre, Robert Jones & Agnes Hunt Orthopaedic Hospital, Oswestry, SY10 7AG, UK

* Address correspondence and reprint requests to:

Ying Yang

Institute of Science & Technology in Medicine

University of Keele

Stoke-on-Trent, ST4 7QB, UK.

E-mail address: y.yang@keele.ac.uk

Abstract

Adult articular chondrocytes are surrounded by a pericellular matrix (PCM) to form a chondron. The PCM is rich in hyaluronan, proteoglycans, collagen II, and it is the exclusive location of collagen VI in articular cartilage. Collagen VI anchors the chondrocyte to the PCM. It has been suggested that co-culture of chondrons with mesenchymal stromal cells (MSCs) might enhance extracellular matrix (ECM) production. This co-culture study investigates whether MSCs help to preserve the PCM and increase ECM production. Primary bovine chondrons or chondrocytes or rat MSCs were cultured alone to establish a baseline level for ECM production. A xenogeneic co-culture monolayer model using rat MSCs (20%, 50% and 80%) was established. PCM maintenance and ECM production were assessed by biochemical assays, immunofluorescence and histological staining. Co-culture of MSCs with chondrons enhanced ECM matrix production, as compared to chondrocyte or chondron only cultures. The ratio 50:50 co-culture of MSCs and chondrons resulted in the highest increase in GAG production (18.5±0.54 pg/cell at day 1 and 11±0.38 pg/cell at day 7 in 50:50 co-culture versus 16.8±0.61pg/cell at day 1 and 10±0.45 pg/cell at day 7 in chondron monoculture). The co-culture of MSCs with chondrons appeared to decelerate the loss of the PCM as determined by collagen VI expression, whilst the expression of high temperature requirement serine protease A1 (HtrA1) demonstrated an inverse relationship to that of the collagen VI. Together this implies that MSCs directly or indirectly inhibited HtrA1 activity and the co-culture of MSCs with chondrons enhances ECM synthesis and the preservation of the PCM.

Key words: chondron, chondrocyte, mesenchymal stromal cells (MSCs), co-culture, collagen VI, HtrA1

Introduction

Adult articular cartilage has a poor capacity for self-repair, with minor injuries often leading to progressive damage and osteoarthritis (Ding et al. 2010). In 1987, cartilage cell therapy was introduced as a treatment for isolated knee articular cartilage defects which might otherwise progress to osteoarthritis (Brittberg et al. 1994). Autologous human chondrocytes were the first source of cells to be used to repair focal cartilage defects. This approach has helped hundreds of patients with an above 80% success rate (Van Osch et al. 2009). In order to advance cartilage cell therapy other cell types are currently being investigated (Burke et al. 2016). One such alternative cell type is the mesenchymal stromal cell (MSC). MSCs are multipotent and can differentiate down a variety of mesenchymal lineages. Adult human MSCs have so far provided mixed results. For example, one observational cohort study reported that adult human MSCs in cartilage repair are as effective as chondrocytes (Nejadnik et al. 2010). Another study reported that the functional properties of native articular cartilage could not be achieved using MSCs alone (Savkovic et al. 2014). The differentiation of adult human MSCs is known to be modulated by growth factors, mechanical stimulation, co-culture with other cells, and interactions with the surrounding extracellular matrix (ECM). Mounting evidence suggests that the co-culture of MSCs with other cell types has great potential in cartilage regeneration (Leijten et al. 2012, Wu et al. 2011; Qing et al. 2011). For example, studies by Wu et al. (2011) and Qing et al. (2011) demonstrated that co-cultures of human MSCs and chondrocytes resulted in enhanced ECM production. The resultant phenotypic changes are considered to be the result of signalling via direct cell–cell contacts, in addition to other parameters generated by the cell types. Other studies have provided evidence in support of co-cultures (Levorson et al. 2014; de Windt et al. 2015). Careful investigation is necessary to unravel the precise role of each of these parameters in the differentiation process.

Within articular cartilage, adult chondrocytes are surrounded by a pericellular matrix (PCM; 2-4 μm thick) to form a chondron (Lee et al. 1997; Chang et al. 1997). The PCM is rich in

hyaluronan, proteoglycans, glycosaminoglycans, collagen II, and it is the exclusive location of collagen VI. Collagen VI anchors the chondrocyte to the PCM by surrounding the cell with a fibrillar basket which intersects at different angles (Fitzgerald and Hansen 2013). This multi-angled configuration ensures that chondrons are stiffer than chondrocytes and better able to withstand loading, as evidenced in our previous work (Wang et al. 2009; 2010). Collagen VI is not degraded by matrix metalloproteinases or by bacterial collagenase but is digested by some serine proteases. HtrA1 is a secretory enzyme and a member of the high temperature requirement family of serine proteases capable of degrading molecules in the PCM (Polur et al. 2010). Polur et al. investigated the co-localisation of HtrA1 with collagen VI in mouse knee cartilage. Collagen VI was absent in chondrocytes expressing HtrA1 suggesting that HtrA1 disrupted the PCM in some way. Thus HtrA1 could be used a tool to study the integrity of the PCM.

It has been suggested that a fully formed PCM prior to chondrocyte implantation is necessary for cartilage tissue engineering (Larson et al. 2002; Vonk et al. 2014). The PCM role is important with both hyaluronan and collagen VI having key roles in development and tissue maturation. A small number of co-culture studies have reported increases in ECM production but, to date, there have been no reports on PCM involvement (de Windt et al. 2015; Vonk et al. 2014). For MSCs, the precise time frame of PCM formation and maturation has yet to be elucidated. In alginate bead culture, Vigfúsdóttir et al. (2010) reported that collagen VI accumulated "regionally" around human MSCs after 1 week and fully enveloped the cells by 2 weeks. There is a need to further our understanding of the role of the PCM in co-cultures. One major drawback to co-culture studies is that they require a large number of cells which cannot be derived from the patient samples obtained at surgery. From our own experience, it is especially difficult to derive large numbers of consistent chondrons from limited supplies of human cartilage. To avoid the issue of cell numbers we utilised well characterised bovine chondrocytes and chondrons following our previously published work (Wang et al. 2009; 2010; 2013). Due to the impracticality of isolating bovine MSCs, we developed a xenogeneic co-culture model using rat MSCs in order to have

sufficient cells to elucidate the effects on collagen VI. Xenogenic co-culture models combining bovine chondrocytes and either rat or rabbit MSCs have been successfully used by a number of other groups without signs of an immune response or other adverse effect (Dahlin RL et al. 2014, Meretoja VV et al. 2014). Thus, the xenogeneic co-culture model using rat MSCs and bovine cartilage cells will have sufficient cells to elucidate the multiple effects on collagen VI. This study initially assessed the morphology and chondrogenic capacity of chondrocytes, chondrons and MSCs in monolayer to develop baseline data. Next chondrocytes or chondrons were co-cultured with different ratios of MSCs to determine whether chondrogenesis could be improved. Our ultimate goal is to determine whether the presence of the MSCs reduces the impact of HtrA1 on the integrity of the PCM.

Material and Methods

Chondrocyte and chondron isolation

Full depth articular cartilage was dissected from the articulating surface of the trochlea humerus of 18-month-old cows. Four separate isolations were performed, each using one humerus. Chondrocyte and chondron isolations were performed with a minor modification of our previously described protocol (Wang et al. 2013). Briefly, diced cartilage was sequentially digested with 0.1% (w/v) proteinase K for 1 hour and then 0.3% (w/v) collagenase type IA for 3 hours. Chondrocytes from the supernatant were strained through a 70 μm cell sieve, washed in Dulbecco's Modified Eagle's Medium (DMEM) supplemented with 10% (v/v) fetal calf serum (FCS). The filtrate was centrifuged at 750 g. The cells were washed three times. For chondron isolation, again four separate isolations were performed, each using one humerus. Diced cartilage was digested with 0.3% (w/v) dispase and 0.2% (w/v) collagenase type XI in DMEM for 5 hour. The cell suspension was filtered through a 70 μm cell sieve, washed in DMEM supplemented with 10% FCS and centrifuged at 750 g. The cells were washed three times. Chondrocytes or

chondrons were either seeded at 1 x10^4 cells per well in 48 well plates (passage 0) or seeded at 2 x 10^4 cells/cm^2 in 25 cm^2 flasks (T25) for monolayer expansion (passage 1).

Rat mesenchymal stromal cells isolation

MSCs were isolated following an established protocol (Mao et al. 2005) in accordance with the animal Act 1986. Briefly, the tibias and femurs from 4-week-old Sprague-Dawley rats were dissected. Both ends of the bones were cut down along the epiphysis, and then the bone marrow was flushed out with 10 mL of cell culture medium consisting of α-minimal essential medium (α-MEM) supplemented with 10% FBS. Bone marrow cells were transferred to a T25 flask and incubated at 37˚C with 5% CO_2. Non adherent cells were removed and media were replaced every three days. P0 and P1 MSCs were used in this study. A tri-lineage differentiation control experiment was conducted according to the protocols (Carvalho et al. 2013) to confirm the MSCs phenotype (Figure 1).

Experimental design

Table 1 summarises our experimental approach involving chondrocytes (CY), chondrons (CN) and mesenchymal stromal cells (MSC). Initial experiments assessed the morphology and the chondrogenic capacity of single cell type cultures in DMEM or α-MEM supplemented with 10% FBS. Follow on experiments assessed the morphology and the chondrogenic capacity of chondrocytes or chondrons co-cultured with MSCs at different ratios in accordance with the literature (Qing et al. 2011). Our experiments were designed to determine the effects of co-culture on morphology and chondrogenesis at P0 and P1. All co-cultures were performed in 48 well-plates at a seeding density of 1x10^4 cells/well. Culture media were replaced every third day and spent media were stored at -20ºC for further analysis. The general morphology, total sulphated glycosaminoglycan (sGAG) content (cell and media), cell number, and the immunolocalisation of key PCM components were assessed at 1, 3, 5 and 7 days in cultures.

Papain digestion for biochemical analysis

At the end of the culture period, the spent culture media and cells were separately digested with 300 μL papain solution per sample for 8 hours at 60°C. Papain solution was prepared by dissolving 125 μg in 0.1 M sodium phosphate, 5 mM EDTA, and 5 mM cysteine-HCL at pH 6.5.

Total sulphated glycosaminoglycan analysis by 1,9-dimethylmethylene blue dye

Total sGAG in spent culture media and cells were assessed separately using the 1,9-dimethylmethylene blue (DMMB) dye assay as previously described (Farndale; Barrett 1986). All reagents were obtained from Sigma. 4 X DMMB solution (32 mg DMMB, 1.52 g glycine, 1.19 g NaCl, 47.5 mL, 0.1 M HCl, pH 3.0) was prepared. Bovine tracheal chondroitin sulphate standards (0-200 μg/mL) were prepared in distilled water. Duplicates (50 μL) of each papain-digested sample and standard were added to a 96-well plate. DMMB (200 μL/well) was added to all wells and the plate was immediately read at 530 nm on a BioTec Synergy 2 plate reader.

Cell number derived from DNA analysis by PicoGreen dye

DNA content was assessed using Picogreen® fluorescent DNA quantification (Molecular Probes, Eugene, OR, USA) as previously described (Wang et al. 2010). The PicoGreen solution was prepared as 1:200 dilutions in 1xTris-EDTA (TE) buffer. Calf thymus DNA standards (Sigma; 0-1 μg/mL) were prepared in distilled water. Fluorescence was determined at 485 nm excitation and 535 nm emission using a plate reader (BioTec Synergy 2). The previously reported value of 7.7 pg of DNA per chondrocyte was used to approximate cell number (Kim et al. 1988).

Histological analysis of proteoglycans

Alcian blue staining was performed to assess the distribution of proteoglycans and their GAGs. At 1, 5 and 7 days, wells were washed with phosphate buffered saline (PBS) and the cell layers were fixed with 4% (v/v) formalin at room temperature for 30 minutes. Formalin was discarded and the wells were washed three times with PBS. The fixed samples were stained with 4% (w/v)

alcian blue solution (pH 2.5) for 30 minutes at room temperature. Excess dye was removed by sequential washing with distilled water. The stained cell layer was left to dry at room temperature prior to viewing under the light microscope (Evos microscope AMEX-1100).

Semi-quantification of cell morphology and GAG staining intensity

The cell morphology was semi-quantified by calculation of cell aspect ratio (length /width) of live cell images through the image analysis using ImageJ software. The length was measured as the longest chord of each cell and the width was the dimension perpendicular to the length. At least 12 cells in each three randomly selected areas were chosen for the calculation. The mean values were collected and plotted for each group and at three culture time points. The intensity of alcian blue staining was semi-quantified using Image J software as well. Briefly, three randomly selected areas from three images were chosen for each group. The integrated intensity tool was used and the mean intensity for different groups and at three culture time points was plotted.

Immunofluorescence staining of the pericellular matrix components

Immunofluorescence staining was performed using primary antibodies against the following components in the PCM: collagen VI (goat polyclonal IgG; Santa Cruz, UK), collagen II (mouse monoclonal IgG; Abcam, UK) and HtrA1 (mouse polyclonal IgG; Santa Cruz, UK). Three samples for each culture group were fixed with 4% (w/v) paraformaldehyde at room temperature for 30 minutes. All samples were subjected to an unmasking treatment prior to the staining in accordance with an established protocol (Wang et al. 2008). Briefly, for detection of collagen VI and collagen II, samples were initially treated with 2 mg/ml testicular hyaluronidase (Sigma). For detection of HtrA1, samples were pre-treated with 25 mU/ml chondroitinase ABC (Sigma) and 2 mg/ml testicular hyaluronidase (Sigma). After pre-treatment, the samples were incubated with the primary antibodies and then labelled with the fluorescein isothiocyanate **(**FITC)-conjugated secondary antibody for collagen II and tetramethylrhodamin (TRITC)-conjugated secondary

antibody for collagen VI and HtrA1 and finally contrast stained with DAP1 to label the nuclei. Articular cartilage was used as a positive control. Primary antibodies were omitted for negative controls. All cells were evaluated using the same exposure time, gain and offset camera settings so that the immunofluorescence intensity was directly comparable among the groups for each given antibody.

Statistical analysis

Biochemical assay results are expressed as the mean±standard deviation (n=3). The Student's two-tailed t test was performed to determine statistical significance (Table 2) with significance defined as $p<0.05$. All statistical analyses were performed using SPSS software.

Results

Cell morphology in 2-dimensional monocultures

The morphology of the individual cell types was assessed up to the end of passage 1 (Figure 2). At passage 0 (Figure 2A, day 1) both chondrocytes and chondrons displayed a predominantly rounded morphology whilst the MSCs had a flat and slightly spread morphology. By day 7, chondrocytes and MSCs had differentiated appearing as fibroblast-like sharp spindles whereas chondrons still retained some degree of rounded morphology. ~~At passage 1 (Figure 2B, day 1) all of the cell types had a similar differentiated fibroblastic-like morphology.~~ At passage 1 (Figure 2B, day 1) and under microscopic observation, all of the cell types had fibroblastic-like morphologies which we would expect to find in monolayer culture.

The differences in cell morphology at passage number 0 between the chondrocytes and chondrons and evolution along culture time and passage number have been further quantified by calculation of the cell aspect ratio (length /width) of live cell images through the image analysis using ImageJ software (Figure 2C). Both chondrons and chondrocytes at day 1 showed round shape morphology with aspect ratio of 1, and the aspect ratio value increased significantly at day

5 and 7 with chondrons having slightly lower aspect ratio value than chondrocytes at each culture time points. MSC showed much higher aspect ratio for all culture time points. Cells at passage number 1 showed similar high aspect ratio values (higher than 1) for all cell types and all culture time points (Data not shown).

Total sulphated GAG production and cell number in 2-dimensional monocultures

The total amount of sulphated GAG accumulated in cells in monoculture was assessed by DMMB at days 1, 3, 5 & 7 (Figure 3A & D). At passage 0 and passage 1, the MSCs did not produce sulphated GAGs whilst the chondrons and chondrocytes accumulated a small amount of sulphated GAGs. Over time the cell number increased for all of the passaged cells (Figure 3B & E). Normalised data confirmed that sulphated GAG production per cell decreased with time and passage which was to be expected in monoculture conditions (Figure 3C & F). GAG production was determined to be 16.8±0.61 pg/cell and 15.4±0.13 pg/cell for chondrons and chondrocytes on day 1, and 10.0±0.45 pg/cell and 10.0±0.51 pg/cell on day 7, respectively. Chondrons had significantly more GAG production than chondrocytes ($p<0.05$). The sGAG products appearing in the media showed slightly different pattern. The chondrocytes demonstrated higher media sGAG content than in cells; whilst chondrons exhibited more GAG in cells than in media. The data are included in the supplement.

Histology in 2-dimensional monocultures

For each cell type, the ECM was stained with alcian blue to detect the presence and distribution of proteoglycans and their GAGs (Figure 4A-B). MSCs did not produce any detectable levels of GAGs throughout the culture period. Typically, the chondrons were more strongly stained than the chondrocytes throughout P0 (Figure 4A). For all culture points of P1 cells, the staining intensity for chondrons and chondrocytes was comparable, and it was less intense than for P0. Semi-quantification of the GAG staining intensity across the groups and culture time by image

analysis software was illustrated in Figure 4C. It is shown that at passage number 0, chondrons presented higher GAG production than chondrocytes at all culture time points significantly and the intensity continuously increases along the culture with significant high GAG at day 7 than day 5 and 3. At passage number 1, both chondrons and chondrocytes presented similar GAG production with less change through prolonged culture. The staining intensity correlated well with the total sulphated GAG (Figure 3).

Immunolocalisation of key PCM components in 2-dimensional monocultures

Figure 5 shows the immunofluorescence staining for PCM markers in the monocultures. MSCs were negative for all PCM markers. For collagen II, the staining intensity increased around chondrons and chondrocytes during P0 and was present, albeit less intense, during P1. Collagen VI, exclusively located in the PCM, was only detected in the chondron cultures. By day 7 (P0), collagen VI staining was lost. For P0 and P1, immunofluorescence staining for HtrA1 was absent for chondrons and chondrocytes at day 1 but present at day 7. At P1, chondrocytes showed stronger HtrA1 staining than the chondrons at the same culture time points. The staining pattern of HtrA1 was inverse to collagen VI staining in P0 chondron. These data were confirmed by comparison with both negative and positive controls using both isolated cells and full depth bovine articular cartilage (supplement data).

Cell morphology in 2-dimensional co-cultures

Two cell type co-cultures were established (Table 1) and cultured to P1, with ratios in agreement with published work (9). We only show the data up to day 7 (P0) since our overall goal was to determine whether different MSC ratios improved the preservation of the PCM as well as the surrounding ECM. Each co-culture was assessed for general cell morphology (Figure 6A-B). Chondrons appeared to maintain a more rounded morphology at all MSC ratios. Chondrocytes appeared more fibroblastic at all MSC ratios. The differences in cell morphology of co-culture MSC between the chondrocytes and chondrons and evolution along culture time have been

quantified by calculation of the cell aspect ratio of live cell images through the image analysis using ImageJ software (Figure 6C). The clear differences were that MSC and chondron co-culture samples had lower aspect ratio value at all culture time point and all cell ratios than mono-culture samples, indicating the improvement of the chondrogenesis by MSC. However the reduction of aspect ratio for MSC and chondrocyte co-culture samples was minimal, and the co-culture samples showed a higher aspect ratio values at day 7.

Total sulphated GAG production and cell number in 2-dimensional co-cultures

Figure 7A illustrates the total amount of GAG accumulated and Figure 7B shows the cell number in co-culture at days 1, 3, 5 & 7. The normalised data confirmed that GAG production per cell decreased with time and passage (Figure 7C), which was with the same trend as in monoculture. MSC and chondron co-cultures increased GAG production. The highest increase was in the samples with 50% MSC ratio. The addition of 50% MSCs increased the GAG production from 16.8±0.61 pg/cell to 18.5±0.54 pg/cell, and from 10.0±0.45 pg/cell to 11±0.38 pg/cell for chondrons at day 1 and day 7, respectively. For chondrocytes, addition of MSCs did not increase the GAG production at any ratio.

Histology in 2-dimensional co-cultures

The co-culture staining for P0 cells by alcian blue is shown in Figure 8a. Chondron co-cultures had more staining for proteoglycans and GAGs than chondrocyte co-cultures. The co-culture 50:50 ratio had the most staining. The quantitative measurement of the GAG staining intensity (Figure 8b) by ImageJ software shows that MSC-chondrons co-culture presented higher GAG than MSC-chondrocyte co-culture at all culture time points and all cell ratio samples significantly and the intensity continuously increased along the culture time with significantly high GAG at day 7 than at day 5 and 3. Both high MSC ratio samples (20% chondron or chondrocyte) showed lowest GAG production.

Immunolocalisation of key PCM components in 2-dimensional co-cultures

For the chondrocyte:MSC co-cultures, there was no collagen VI staining at any time points or ratio. For all chondron:MSC co-cultures, collagen VI was detected for all time points and ratios (Figure 9). Collagen VI staining was most intense in the 50% chondron:MSC co-cultures which correlated with the alcian blue staining (Figure 8). At P0, both chondron and chondrocyte co-cultures showed collagen II staining increase from day 1 to day 7. The most intense staining was at the 50% ratio. HtrA1 staining was, in general, lower than monoculture in all co-culture ratios across chondrons and chondrocytes. There was no visible staining of HtrA1 in 50% chondrons:MSC co-cultures and at all culture time point. The strongest staining was in the samples of chondrocyte:MSC co-cultures at day 7.

Discussion

Recent studies have suggested that a fully formed PCM is necessary for cartilage tissue engineering (Vonk et al. 2010). For freshly isolated chondrocytes in 3-dimensional culture, the PCM takes 1 week to form and then a further 11 weeks to remodel. One can speculate that one of the advantages of chondrons over chondrocytes for cell therapy applications is that, at the time of their implantation, chondrons would be 12 weeks further along with respect to cartilage ECM formation. Recent work in a goat model has shown that human chondrons produce more cartilage ECM than human chondrocytes, when cultured with human MSCs (Bekkers et al. 2013). Herein we have set out experiments to investigate whether chondrons produce more ECM when co-cultured with MSCs. To circumvent the low yield of chondrons from small “off cuts” of patient tissue we have developed a xenogeneic co-culture model using rat MSCs. Our monolayer culture model is in no way perfect but it does offer an interesting insight into chondrocyte and chondron co-cultures and the benefit mechanism of MSC. Work still remains to be done to optimise the ratio of chondrons to human MSCs and to fully characterise the cartilage ECM that they produce.

Our data suggests that MSCs have the potential to help preserve the PCM and improve the deposition of ECM in a dose response style.

The PCM can be primarily defined by a layer of collagen VI at the cell surface and lesser expression of collagen II. We detected collagen II and IV in our chondron monoculture model. Only collagen II was detected in our chondrocyte monolayer model. In our model, isolated chondrons maintained a round shape and collagen VI staining until day 5 whilst isolated chondrocytes showed a rapid morphological change becoming irregular and elongated. By P1, there was no collagen VI staining at all culture time points and across chondron and chondrocyte. Collagen VI is one of the major components of the pericellular matrix network. Thus, the disappearance of type VI collagen from the pericellular matrix is a good indicator that the pericellular matrix network has been disturbed. Our monoculture model clearly demonstrated that PCM was degraded rapidly in monolayer culture.

There are gaps in our understanding of PCM degradation. Mammalian HtrA1 is a secreted member of the trypsin family of serine proteases which has the potential to degrade the PCM (Polur et al. 2010). It has been reported that collagen VI was absent from chondrocytes expressing HtrA1 in mouse OA joints, which is indicative of the disruption of the PCM (Hou et al. 2013). On the other hand, in an in vitro alginate hydrogel culture model, collagen VI was detected in the PCM whilst HtrA1 expression was absent (Polur et al. 2010). Our chondron monoculture model further confirmed the inverse relationship between the expression of HtrA1 and collagen VI. Thus, the presence of HtrA1 could be a crucial to the degradation of collagen VI. Inhibition of HtrA1 production or inactivation of HtrA1 could protect collagen VI and preserve the integrity of PCM.

Originally, we hypothesised MSCs would improve chondrogenic phenotype in co-culture with chondrons or chondrocytes. Several laboratories have reported that co-cultures of MSCs and chondrocytes enhance chondrogenesis (Levorson et al. 2014; Meretoja et al. 2012). These studies

led us to investigate the relation between MSC ratios and HtrA1 production, and ECM synthesis in co-culture. As seen in Figure 9, HtrA1 immunostaining was considerable lower in our co-culture model than in monoculture samples. No visible staining of HtrA1 in 50% chondron:MSC at all culture time points. Consequently, higher collagen VI staining was evident in all MSC:chondron cultures. It is not surprising that MSC:chondrocyte co-culture did not show any collagen VI staining at all ratios and at all culture time points since the PCM was not present or induced in our culture model. Hence, we speculate that MSCs directly or indirectly suppressed the production of HtrA1 or generated inhibitor for HtrA1 in co-culture, leading to the preservation and promotion of PCM.

In our co-culture model, MSCs improved the chondrogenesis manifested as the increase of collagen II and sGAG production in all ratio of co-culture with chondrons in comparison to monoculture. The underlying mechanism could be via trophic factors secreted by MSCs. Uniquely, we did not used chondrogenic media in this co-culture study, which created an environment to reveal the intrinsic interaction of MSCs and cartilage cells with and without PCM. It has been report that chondrogenic media induce MSC hypertrophy (Hubka et al. 2014). Our results suggest that 50% chondrons cultured with 50% MSC resulted in the most significant increase in chondrogenesis. There have been fewer investigations into co-cultures of MSCs and chondrons (de Windt et al. 2015; Nikpou et al. 2016). Our co-culture was slightly different to Nikpou et al. who used indirect chondrons co-culture and used a nanofiber scaffold. In addition, Nikpou et al. used chondrons from osteoarthritis patients. We believe that this enhancement is most likely due to the positive effect that is conveyed by the PCM. It is possible that MSC prolong collagen VI expression by chondrons but further experiments are needed to confirm our hypothesis.

In conclusion, our data suggests that together chondrons and MSC improve ECM production and demonstrated ability to maintain the PCM. The inverse expression of HtrA1 and collagen VI

supports our hypothesis that the MSCs secreted inhibition factor(s) for HtrA1 which was responsible for the degradation of components of the PCM. The ratio of 50:50 of MSCs in co-culture with chondrons presented the highest potential for further development in cartilage regeneration. The benefit effect of MSC and chondrocytes in our study was minimal. These data may enable us to improve upon current cell therapies through a more defined combination of chondrons and MSCs.

Acknowledgement: The authors thank Miss Katy Cressy and Mr John Misra in GHRC, Keele University for their technical support.

Conflict of Interest: The authors declare that there is no conflict of interest.

References

Bekkers JE, Tsuchida AI, van Rijen MH, Vonk LA, Dhert WJ, Creemers LB, Saris DB (2013) Single-stage cell-based cartilage regeneration using a combination of chondrons and mesenchymal stromal cells: comparison with microfracture. Am J Sports Med 41:2158-2166.

Brittberg M, Lindahl A, Nilsson A, Ohlsson C, Isaksson O, Peterson L (1994) Treatment of deep cartilage defects in the knee with autologous chondrocyte transplantation. N Eng J Med 331:889-895.

Burke J, Hunter M, Kolhe R, Isales C, Hamrick M, Fulzele S (2016) Therapeutic potential of mesenchymal stem cell based therapy for osteoarthritis. Clin Transl Med 5:27-016-0112-7.

Carvalho AdM, Yamada ALM, Golim M, Álvarez L, Jorge L, Conceição M, Deffune E, Hussni CA, Alves A (2013) Characterization of mesenchymal stem cells derived from equine adipose tissue. Arq. Bras. Med. Vet. Zootec 65:939-945.

Chang J, Poole CA (1997) Confocal analysis of the molecular heterogeneity in the pericellular microenvironment produced by adult canine chondrocytes cultured in agarose gel. Histochem J 29:515-528.

Dahlin RL, Kinard LA, Lam J, Needham CJ, Lu S, Kasper FK, Mikos AG (2014) Articular chondrocytes and mesenchymal stem cells seeded on biodegradable scaffolds for the repair of cartilage in a rat osteochondral defect model. Biomaterials 35:7460-7469.

de Windt TS, Saris DB, Slaper-Cortenbach IC, van Rijen MH, Gawlitta D, Creemers LB, de Weger RA, Dhert WJ, Vonk LA (2015) Direct cell–cell contact with chondrocytes is a key mechanism in multipotent mesenchymal stromal cell-mediated chondrogenesis. Tissue Eng Part A 21:2536-2547.

de Windt TS, Vonk LA, Slaper-Cortenbach IC, van den Broek MP, Nizak R, van Rijen MH, de Weger RA, Dhert WJ, Saris DB (2017) Allogeneic Mesenchymal Stem Cells Stimulate Cartilage Regeneration and Are Safe for Single-Stage Cartilage Repair in Humans upon Mixture with Recycled Autologous Chondrons. Stem Cells 35:256-264.

Ding C, Jones G, Wluka AE, Cicuttini F (2010) What can we learn about osteoarthritis by studying a healthy person against a person with early onset of disease? Curr Opin Rheumatol 22:520-527.

Farndale RW, Buttle DJ, Barrett AJ (1986) Improved quantitation and discrimination of sulphated glycosaminoglycans by use of dimethylmethylene blue. Biochim Biophys Acta 883:173-177.

Fitzgerald J, Holden P, Hansen U (2013) The expanded collagen VI family: new chains and new questions. Connect Tissue Res 54:345-350.

Hou Y, Lin H, Zhu L, Liu Z, Hu F, Shi J, Yang T, Shi X, Zhu M, Godley BF (2013) Lipopolysaccharide Increases the Incidence of Collagen‐Induced Arthritis in Mice Through Induction of Protease HTRA‐1 Expression. Arthritis Rheum 65:2835-2846.

Hubka KM, Dahlin RL, Meretoja VV, Kasper FK, Mikos AG (2014) Enhancing chondrogenic phenotype for cartilage tissue engineering: monoculture and coculture of articular chondrocytes and mesenchymal stem cells. Tissue Eng Part B 20:641-654.

Kim YJ, Sah RL, Doong JY, Grodzinsky AJ (1988) Fluorometric assay of DNA in cartilage explants using Hoechst 33258. Anal Biochem 174:168-176.

Larson CM, Kelley SS, Blackwood AD, Banes AJ, Lee GM (2002) Retention of the native chondrocyte pericellular matrix results in significantly improved matrix production. Matrix Biol 21:349-359.

Lee GM, Loeser RF (1998) Interactions of the chondrocyte with its pericellular matrix. Cells Mater 8:135-149.

Lee GM, Poole CA, Kelley SS, Chang J, Caterson B (1997) Isolated chondrons: a viable alternative for studies of chondrocyte metabolism in vitro. Osteoarthritis Cartilage 5:261-274.

Leijten JC, Georgi N, Wu L, van Blitterswijk CA, Karperien M (2013) Cell sources for articular cartilage repair strategies: shifting from monocultures to cocultures. Tissue Eng Part B 19:31-40.

Levorson EJ, Santoro M, Kasper FK, Mikos AG (2014) Direct and indirect co-culture of chondrocytes and mesenchymal stem cells for the generation of polymer/extracellular matrix hybrid constructs. Acta Biomater 10:1824-1835.

Mao X, Chu CL, Mao Z, Wang JJ (2005) The development and identification of constructing tissue engineered bone by seeding osteoblasts from differentiated rat marrow stromal stem cells onto three-dimensional porous nano-hydroxylapatite bone matrix in vitro. Tissue Cell 37:349-357.

Meretoja VV, Dahlin RL, Kasper FK, Mikos AG (2012) Enhanced chondrogenesis in co-cultures with articular chondrocytes and mesenchymal stem cells. Biomaterials 33:6362-6369.

Meretoja VV, Dahlin RL, Wright S, Kasper FK, Mikos AG (2014) Articular chondrocyte redifferentiation in 3D co-cultures with mesenchymal stem cells. Tissue Eng Part C 20:514-523.

Nejadnik H, Hui JH, Feng Choong EP, Tai B, Lee EH (2010) Autologous bone marrow–derived mesenchymal stem cells versus autologous chondrocyte implantation: an observational cohort study. Am J Sports Med 38:1110-1116.

Nikpou P, Nejad DM, Shafaei H, Roshangar L, Samadi N, Navali AM, Sadegpour AR, Shanehbandi D, Rad JS (2016) Study of chondrogenic potential of stem cells in co-culture with chondrons. Iran J Basic Med Sci. 19:638.

Polur I, Lee PL, Servais JM, Xu L, Li Y (2010) Role of HTRA1, a serine protease, in the progression of articular cartilage degeneration. Histol Histopathol 25:599-608.

Qing C, Wei-ding C, Wei-min F (2011) Co-culture of chondrocytes and bone marrow mesenchymal stem cells in vitro enhances the expression of cartilaginous extracellular matrix components. Braz J Med Biol Res. 44:303-310.

Savkovic V, Li H, Seon J, Hacker M, Franz S, Simon J (2014) Mesenchymal stem cells in cartilage regeneration. Curr Stem Cell Res T 9:469-488.

Twomey J, Thakore P, Hartman D, Myers E, Hsieh A (2014) Roles of type VI collagen and decorin in human mesenchymal stem cell biophysics during chondrogenic differentiation. Eur Cell Mater 27:237-250.

Van Osch GJ, Brittberg M, Dennis JE, Bastiaansen‐Jenniskens YM, Erben RG, Konttinen YT, Luyten FP (2009) Cartilage repair: past and future–lessons for regenerative medicine. J Cell Mol Med 13:792-810.

Vigfúsdóttir ÁT, Pasrija C, Thakore PI, Schmidt RB, Hsieh AH (2010) Role of pericellular matrix in mesenchymal stem cell deformation during chondrogenic differentiation. Cell Mol Bioeng 3:387-397.

Vonk LA, de Windt T, Kragten A, Beekhuizen M, Mastbergen S, Dhert W, Lafeber F, Creemers L, Saris D (2014) Enhanced cell-induced articular cartilage regeneration by chondrons; the influence of joint damage and harvest site. Osteoarthritis Cartilage 22:1910-1917.

Vonk LA, Doulabi BZ, Huang C, Helder MN, Everts V, Bank RA (2010) Preservation of the chondrocyte's pericellular matrix improves cell‐induced cartilage formation. J Cell Biochem 110:260-271.

Wang Q, Hughes N, Cartmell S, Kuiper N (2010) The composition of hydrogels for cartilage tissue engineering can influence glycosaminoglycan profile. Eur Cell Mater 19:b93.

Wang QG, El Haj AJ, Kuiper NJ (2008) Glycosaminoglycans in the pericellular matrix of chondrons and chondrocytes. J Anat 213:266-273.

Wang QG, Magnay JL, Nguyen B, Thomas CR, Zhang Z, El Haj AJ, Kuiper NJ (2009) Gene expression profiles of dynamically compressed single chondrocytes and chondrons. Biochem Biophys Res Commun 379:738-742.

Wang QG, Nguyen B, Thomas CR, Zhang Z, El Haj AJ, Kuiper NJ (2010) Molecular profiling of single cells in response to mechanical force: comparison of chondrocytes, chondrons and encapsulated chondrocytes. Biomaterials 31:1619-1625.

Wu L, Prins H, Helder MN, van Blitterswijk CA, Karperien M (2012) Trophic effects of mesenchymal stem cells in chondrocyte co-cultures are independent of culture conditions and cell sources. Tissue Eng Part A 18:1542-1551.

Figure captions

Figure 1: Illustration of Tri-lineage staining images after 21 days culture of MSC positive control. (A) Adipose differentiated cells (Red oil staining); (B) osteoblast differentiated cells (Alizarin red); (C) chondrogenic differentiated cells (Toluidine Blue). Scale bar represents 150 µm.

Figure 2: Cell morphology of chondrons (CN), chondrocytes (CY) or MSCs in monolayer culture at Days 1, 5 and 7 at (A) P0 and (B) P1. The scale bars represent 80 µm. (C) Cell aspect ratio analysis of P0 chondron (CN) and chondrocyte (CY) in monoculture at day 1, 5, and 7. Data are expressed as mean±SD (n=3). (*) Statistically significant difference between day 7 and day 5, (x) statistically significant difference between day 7 and day 1, (^) statistically significant difference between day 5 and day 1 and (#) statistically significant difference between CN, CY and MSC at day 7.

Figure 3: sGAG and cell number analysis of chondron (CN), chondrocyte (CY) or MSC in monoculture at Days 1, 3, 5 and 7 at P0 (Panels A-C) and P1 (Panels D-F). Panel A & D represent total sGAG production in cells. Panel B & E represent total cell number. Panel C & F represent total sGAG production normalised to cell number. Data are expressed as mean±SD (n=3).

Figure 4: Representative images of alcian blue stained monocultures of chondrons (CN), chondrocytes (CY) or MSC at Days 1, 5 and 7 at (A) P0 and (B) P1. The scale bars represent 150 µm. (C) Alcian blue staining of chondron (CN), chondrocyte (CY) and MSC in monoculture at day 1, 5 and 7 at (A) P0 and (B) P1. Data are expressed as mean±SD (n=3). (*) Statistically significant difference between day7 and day 5, (x) statistically significant difference between day 7 and day 1, (^) statistically significant difference between day 5 and day 1 and (#) statistically significant difference between CN and CY at day 7.

Figure 5: Representative immunofluorescently stained images of chondrons (CN), chondrocytes (CY) or MSCs at Days 1, 5 and 7 at P0 (Panels A-C) and P1 (Panels D-F). The cells were stained for (A & D): collagen VI (green); (B & E): collagen II (red) and (C & F): HtrA1 (red). The cells were counter-stained by DAPI (blue). The white arrows indicate positive staining. The scale bars represent 20 μm.

Figure 6: Cell morphology of co-culture of chondrons (CN, Panel A) or chondrocytes (CY, Panel B) with MSCs in accordance with the ratios shown in Table 1. Co-cultures were assessed at Days 1, 5 and 7 at P0. The scale bars represent 80 μm. (C) Cell aspect ratio analysis of P0 chondron (CN) and chondrocyte (CY) in co-culture with MSC at different ratios at Days 1, 5, and 7. Data are expressed as mean±SD (n=3). (*) Statistically significant difference between day 7 and day 5, (x) statistically significant difference between day 7 and day 1, (^) statistically significant difference between day 5 and day 1 and (#) statistically significant difference between different ratios at day 7.

Figure 7: sGAG and cell number analysis of chondron (CN; Panels A-C) or chondrocyte (CY; Panels D-F) with MSC in co-culture at Days 1, 3, 5 at P0. (A, D) total sGAG production in cells; (B, E) total cell number; (C, F) the total sGAG production normalised to cell number. Data are expressed as mean±SD (n=3).

Figure 8: (A) Representative images of alcian blue stained chondrons (CN) or chondrocytes (CY) with MSC in co-culture at Days 1, 5 and 7 at P0. The scale bars represent 150 μm. (B) Alcian blue staining intensity of P0 chondron (CN) and chondrocyte (CY) in co-culture with MSC at different ratios at days 1, 5, and 7. Data are expressed as mean±SD (n=3). (*) Statistically significant difference between day 7 and day 5, (x) statistically significant difference between day 7 and day 1, (^) statistically significant difference between day 5 and day 1 and (#) statistically significant difference between different ratios at day 7.

Figure 9: Representative immunofluorescently stained images of chondrons (CN) or chondrocytes (CY) co-cultured with MSCs at Days 1, 5 and 7 at P0. The cells were stained for (A): collagen VI (green); (B): collagen II (red); (C): HtrA1 (red). The cells were counter-stained by DAPI (blue). The white arrows indicate positive staining. The scale bars represent 20 μm.

Supplement figures

Figure SI: Immunofluorecence staining images of positive and negative controls. Positive control: freshly dissected bovine cartilage; negative control: staining without primary antibodies. (A) Collagen VI (green); (B) Collagen II (red); (C) HtrA1 (red). The cells were counter-stained by DAPI (blue). Scale bars represent 20μm.

Figure SII: Illustration of freshly dissected bovine cartilage stained by alcian blue. Scale bars represent 150 μm.

Figure SIII sGAG production in media and in cells for monoculture (chondron (CN) and chondrocyte (CY)) and co-culture with 20, 50, 80% of MSC ratio at day 1, 3, 5, 7 at P0 cells.

Table 1: Description of experimental groups with cell types and densities seeded.

Table 2: Definition of symbols representing statistical significance ($p < 0.05$).

Experimental group	Chondrocytes per well	Chondrons per well	MSCs per well
CY	10,000	-	-
CY 80	8,000	-	2,000
CY50	5,000	-	5,000
CY20	2,000	-	8,000
CN	-	10,000	-
CN80	-	8,000	2,000
CN50	-	5,000	5,000
CN20	-	2,000	8,000
MSC	-	-	10,000

Table 1: Description of experimental groups with cell types and densities seeded.

Symbol	Meaning
*	Statistically significant difference between MSCs and chondrocytes
X	Statistically significant difference between MSCs and chondrons
+	Statistically significant difference between chondrocytes and chondrons
&	Statistically significant difference between 80% and 20% co-culture ratios for the same cell type
^	Statistically significant difference between 50% and 20% co-culture ratios for the same cell type
#	Statistically significant difference between 80% and 50% co-culture ratios for the same cell type

Table 2: Definition of symbols representing statistical significance ($p < 0.05$).

Figure 1

Click here to download Figure Figure 1 HOwida.tif

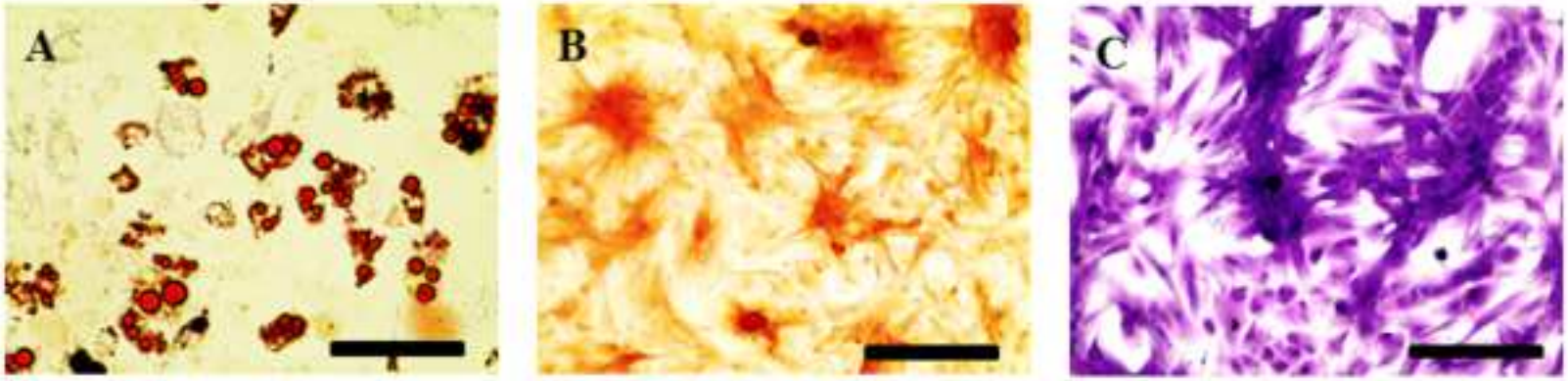

Figure 2

Click here to download Figure Figure 2 HOwida.tif

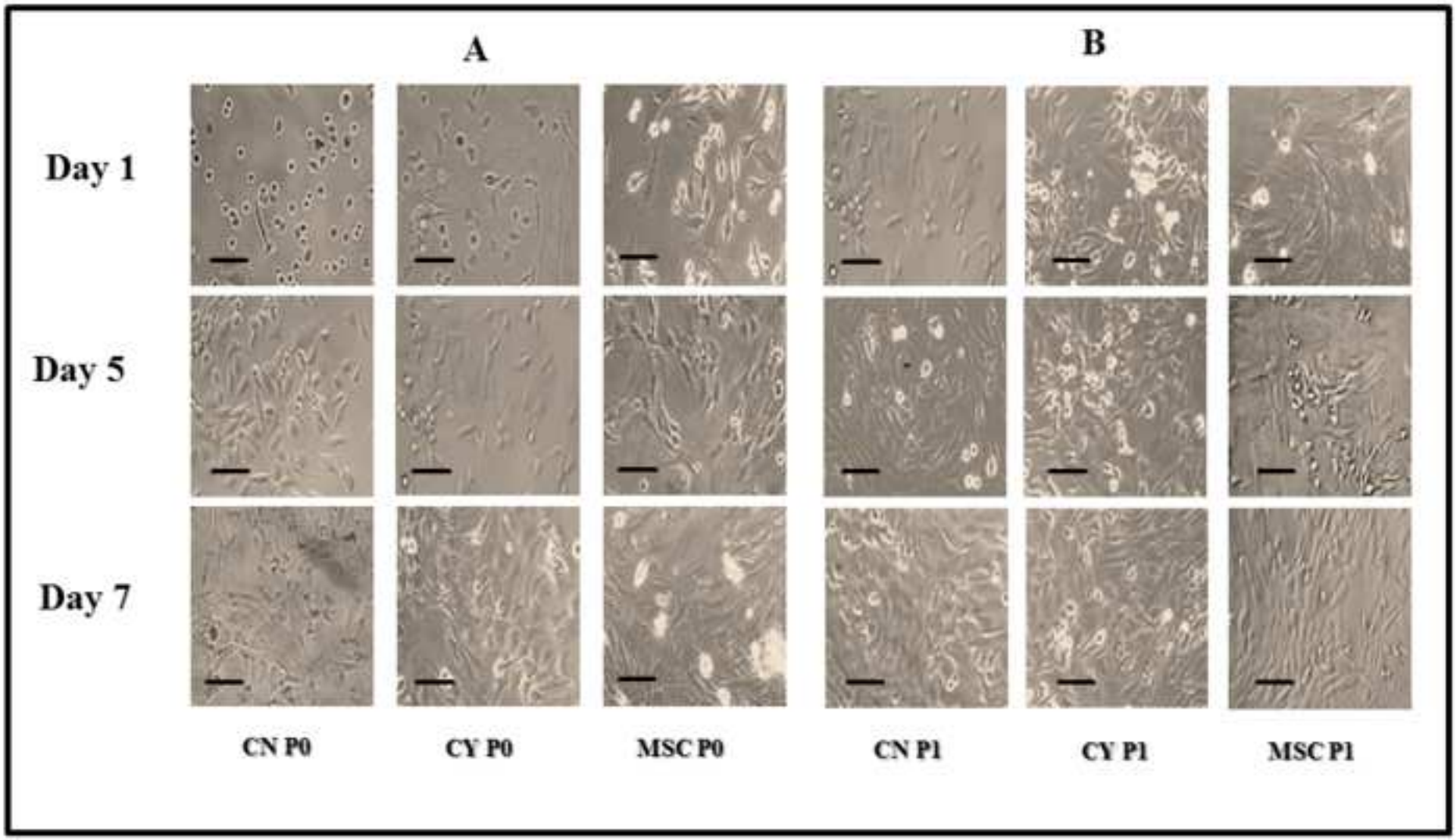

Figure 2C

Click here to download Figure Figure 2C HOwide.tif

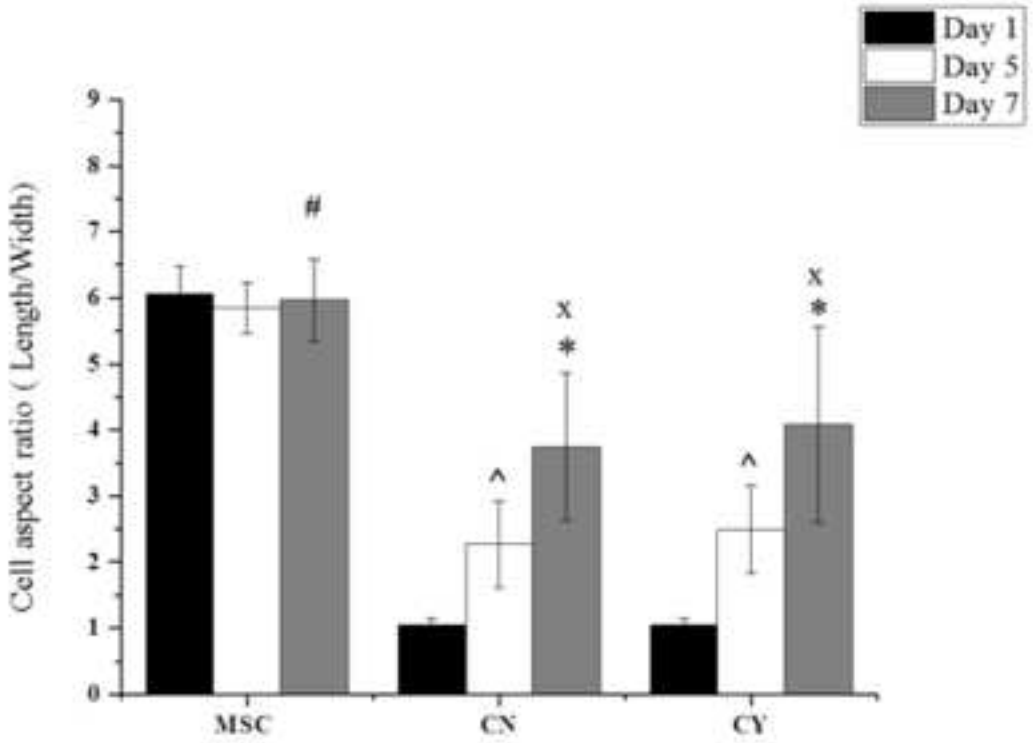

Figure 2C

Figure 3

Click here to download Figure Figure 3 HOwida.tif

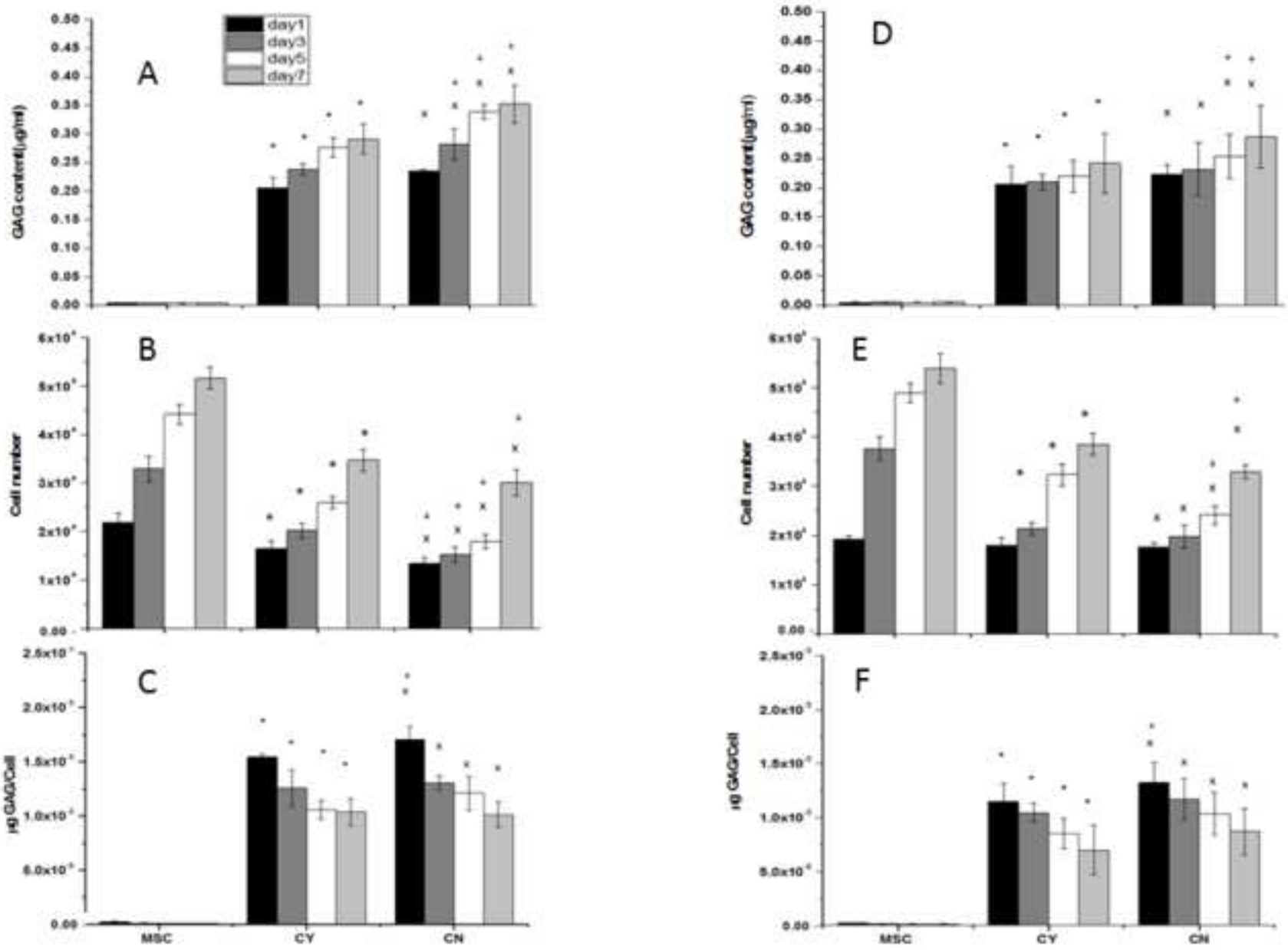

Figure 4

Click here to download Figure Figure 4 HOwida.tif

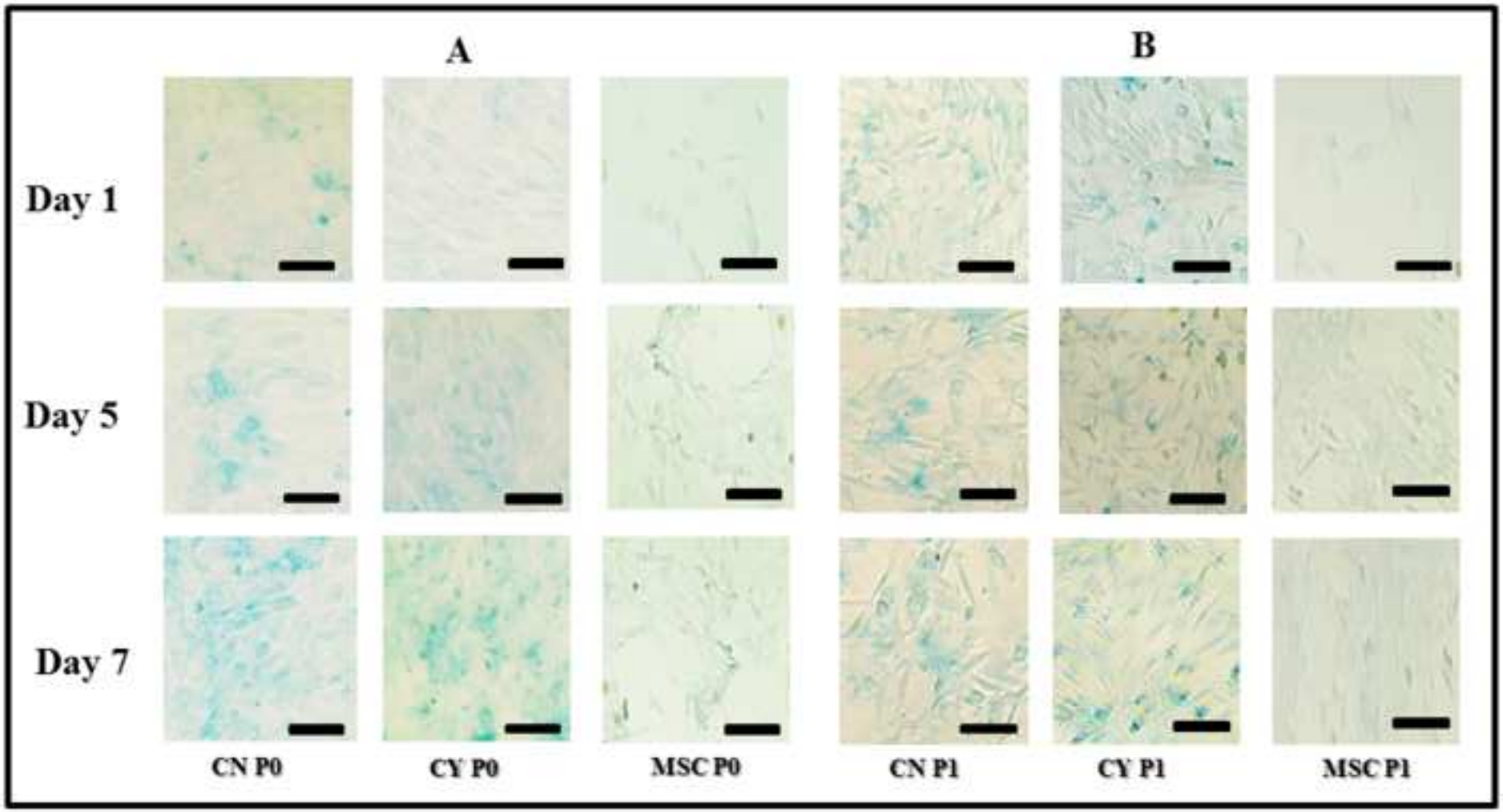

Figure 4C

Click here to download Figure Figure 4C HOwide.tif

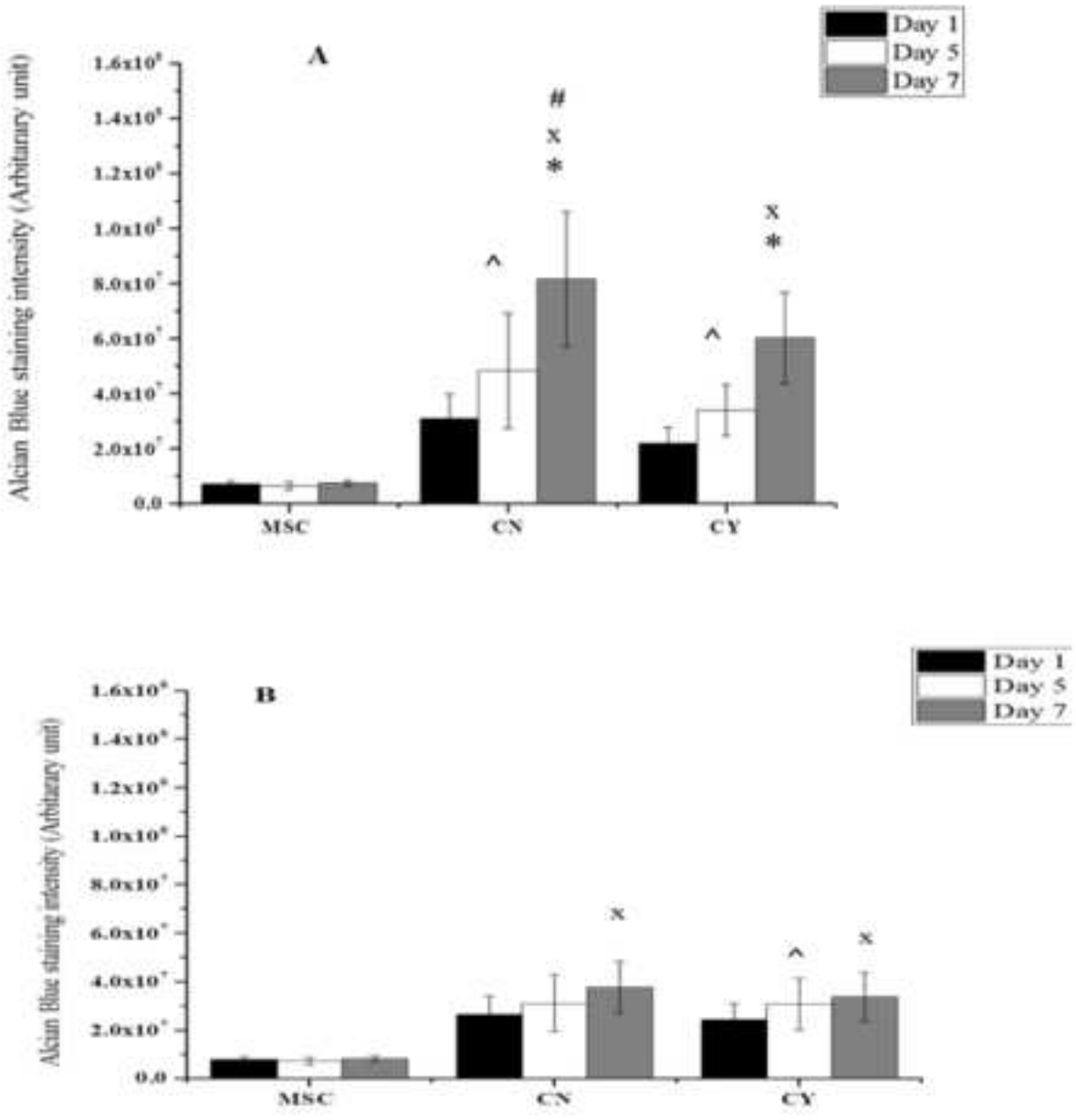

Figure 4C

Figure 5

Click here to download Figure new Figure 5 HOwida.tif

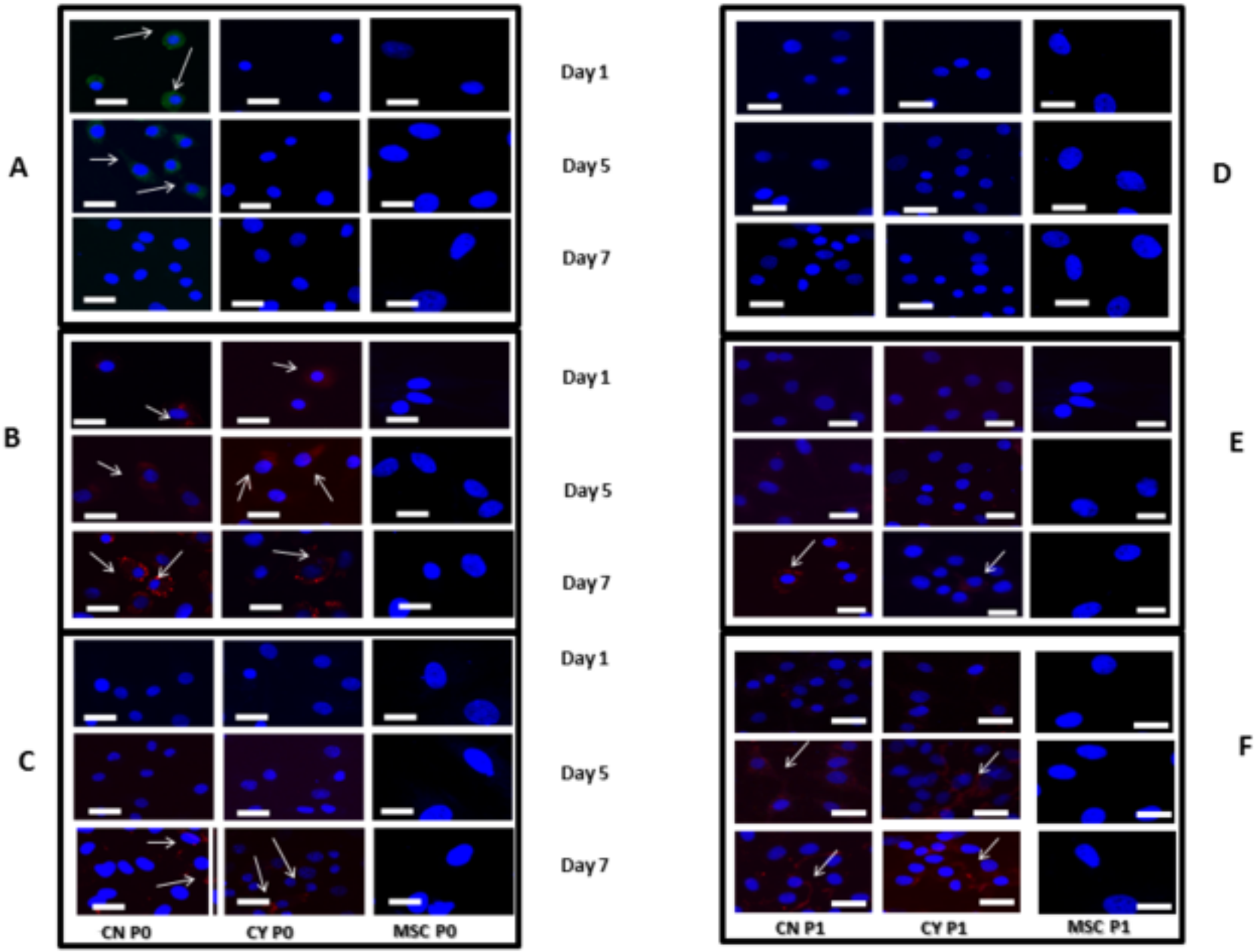

Figure 6

Click here to download Figure Figure 6 HOwida.tif

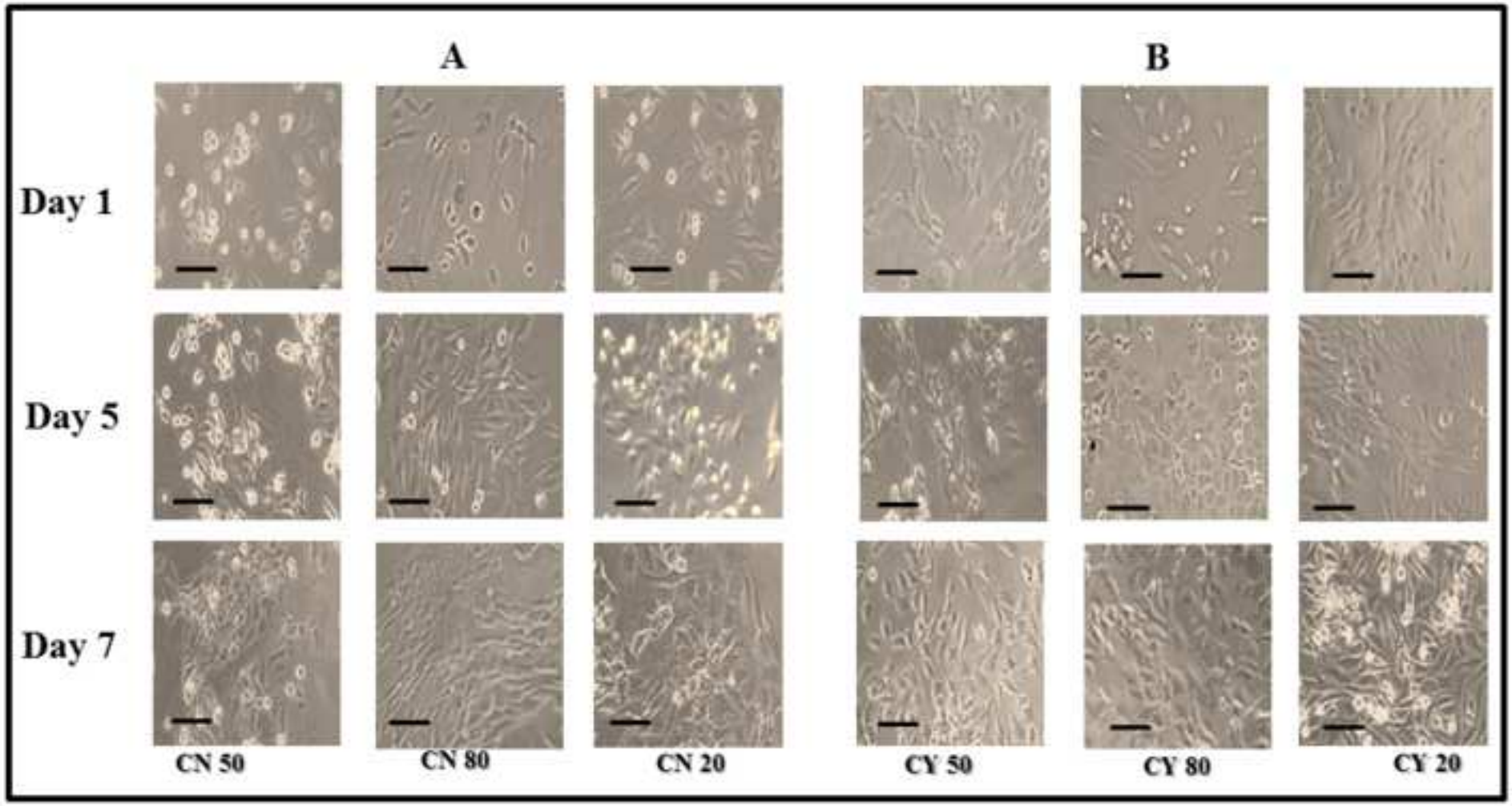

Figure 6C

Click here to download Figure Figure 6C HOwide.tif

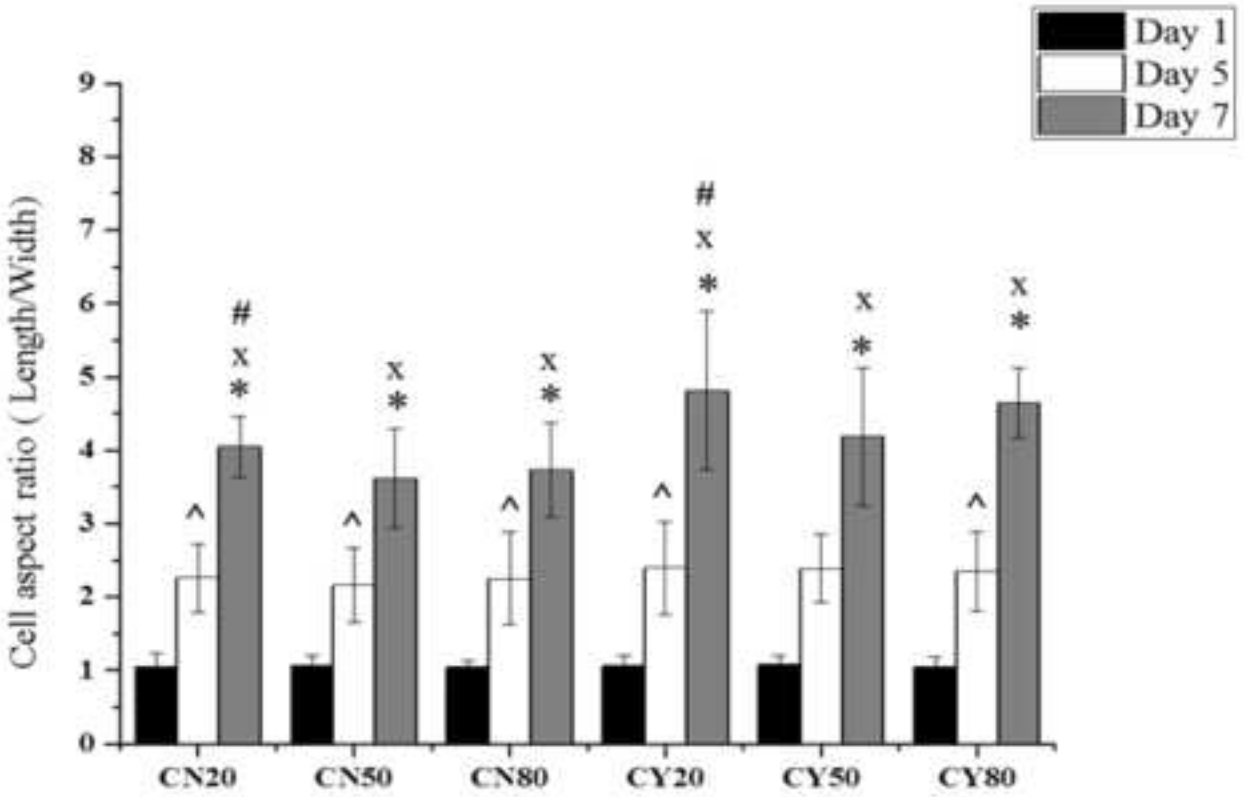

Figure 6C

Figure 7

Click here to download Figure Figure 7 HOwida.tif

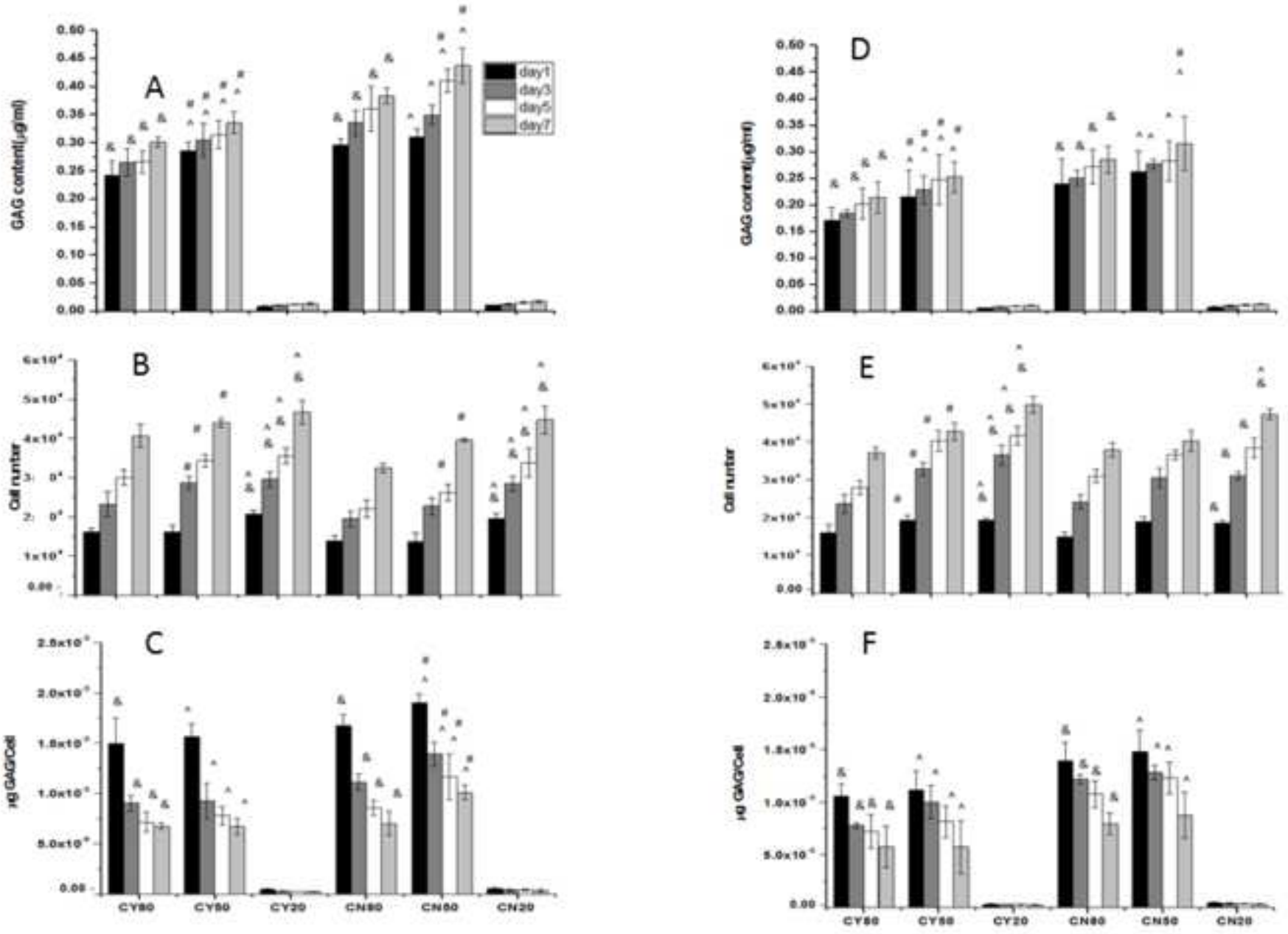

Figure 8

Click here to download Figure Figure 8 HOwida.tif

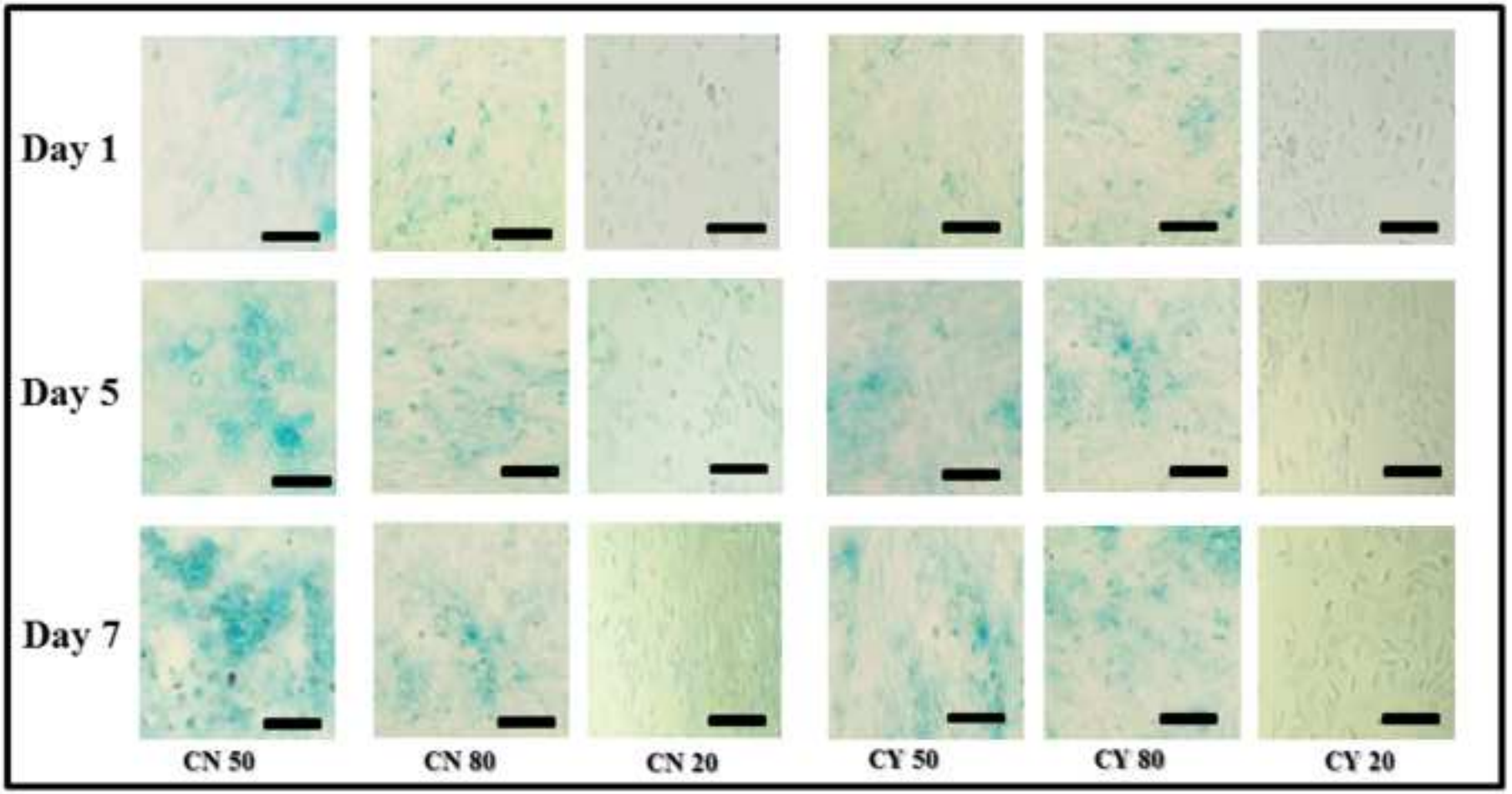

Figure 8B

Click here to download Figure Figure 8b HOwide.tif

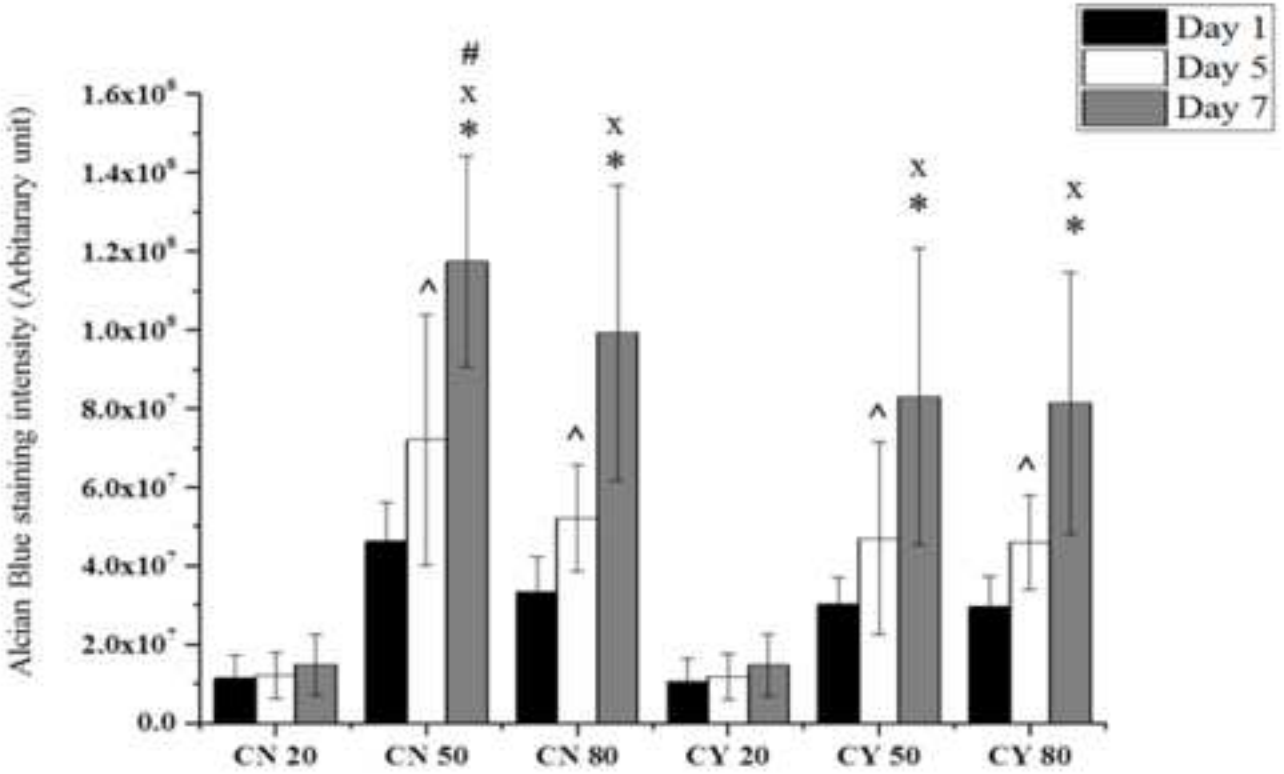

Figure 8b

Figure 9

Click here to download Figure Figure 9 HOwida.tif

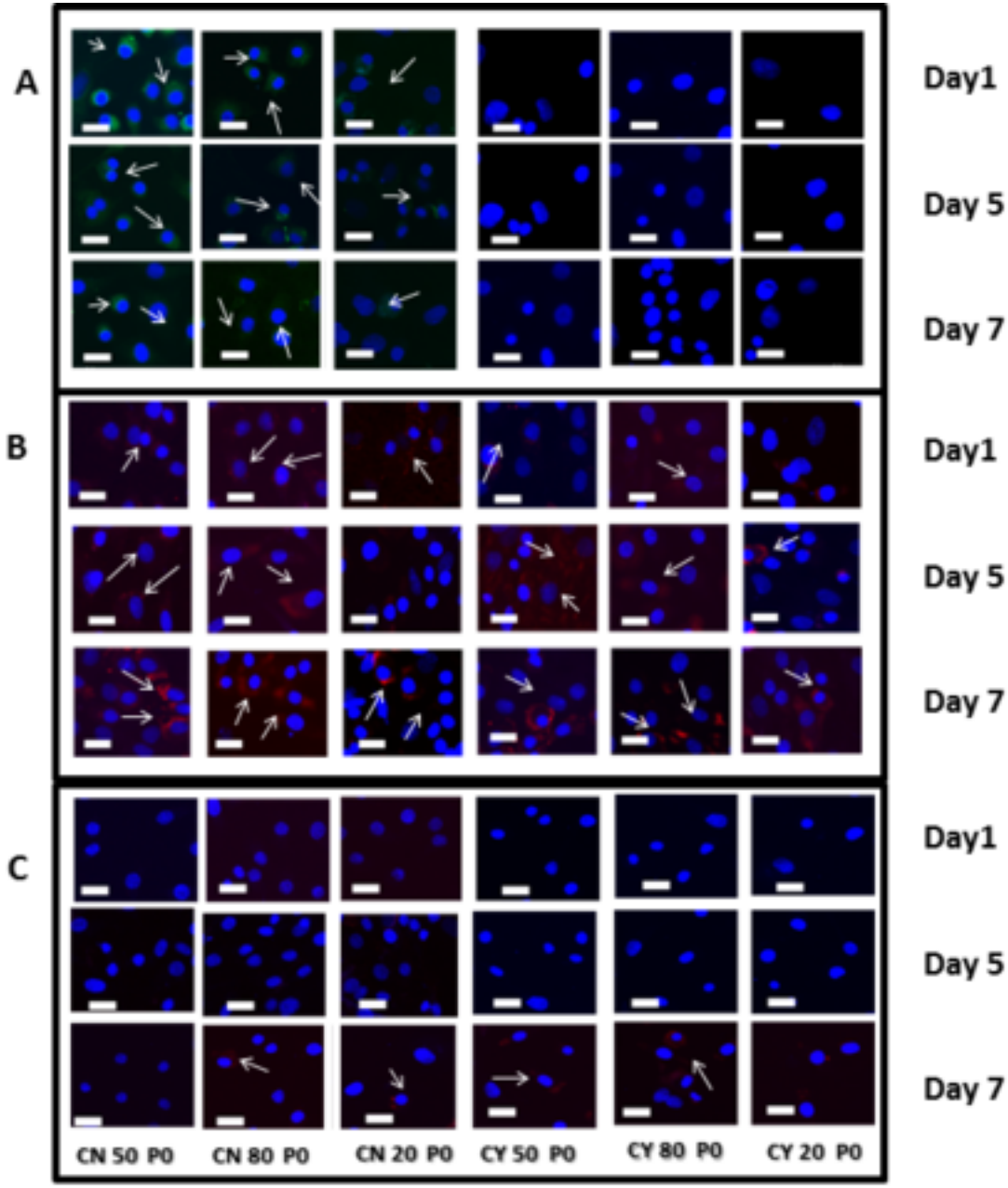

Supplementary Figure SI

Supplementary Figure SII

Supplementary Figure SIII